

Transition zone studies of vegetable fibre–cement paste composites

Holmer Savastano Jr.,* Vahan Agopyan

University of Sao Paulo, P.O. Box 23, 13630-000 Pirassununga SP, Brazil

Received 12 November 1997; accepted 27 August 1998

Abstract

The transition zone of short filament fibres randomly dispersed in a paste of ordinary Portland cement was analysed. Composites with vegetable fibres (malva, sisal and coir) were compared with those with chrysotile asbestos and polypropylene fibres. The composites were prepared for testing at the ages of 7, 28, 90 and 180 days. The water–cement ratio was 0.38; at the age of 28 days specimens with $w/c = 0.30$ and a $w/c = 0.46$ were also tested. Mechanical tests evaluated the composite tensile strength and ductility. Backscattered electron imaging (BSEI) and energy dispersive spectroscopy (EDS) were used to identify the major properties of the fibre–matrix interface. Mainly for vegetable fibre composites the transition zone is porous, cracked and rich in calcium hydroxide macrocrystals. These characteristics are directly related to the fibre–matrix bonding and to the composite mechanical performance. © 1999 Elsevier Science Ltd. All rights reserved.

Keywords: Transition zone; Vegetable fibres; Asbestos fibres; Polypropylene fibres; Composites; Fibre–cement

1. Introduction

According to the suggestions of various researchers [1–3], the presence of reinforcement (steel, aggregates or impermeable fibres) in cement paste creates a wall effect, that is, the formation of a water film at the interface. This assumption is used to explain the greater porosity and the concentration of portlandite crystals (calcium hydroxide) and of ettringite (hydrated calcium trisulfoaluminate) near the interface, and that defines the transition zone, with characteristics much different from the rest of the matrix [4].

The significance of the interfacial transition zone is well established for interfaces between cement paste and impermeable inclusions [5], but it is not so clear that the same principles apply to permeable phases such as natural fibres.

The importance of vegetable fibres is in their availability in Brazil and in other countries with agricultural based economies.

This research analyses the basic characteristics of the transition zone between Portland cement paste and porous vegetable fibres of malva, sisal and coir, in comparison with mineral fibres of chrysotile asbestos and polypropylene. The influence of the water–cement

ratio of the matrix and the age of the composite, on the characteristics of the transition zone is also evaluated and correlated to mechanical properties of the composite.

1.1. Transition zone

Majumdar and Ryder [6] presented some important studies concerning cement pastes reinforced with Cem-FIL glass fibres (high zirconium glass), which were more resistant to the alkalis of cement matrix than the ordinary E-glass fibres (aluminaborosilicate glass). Experiments were carried out with scanning electron microscopy (SEM) and with X-ray microanalysis, registering the evolution of hydrated products in relation to time and the increase of portlandite on the fibre surface.

The research of Bentur et al. [7], with steel fibres aligned in a cement paste matrix, indicated that cracks tend to accompany the transition zone, at a distance of approximately 40 μm from the fibre surface. These observations were also made with the SEM.

In another study regarding the transition zone evolution in cement composites with cellulose fibres, Bentur and Akers [8] registered the increase of the porosity and the concentration of portlandite in the early hydration stages. After that, various ageing conditions were applied and petrification of fibres was observed. This

*Corresponding author. Tel.: +55 19 561 2044; fax: +55 19 561 1689; e-mail: holmersj@usp.br

petrification occurred under adequate conditions of carbonation by the filling of the lumen of the fibre bundles with the hydration products. They found that the tensile strength of the aged composite was reduced, accompanied by the predominance of fibres breaking.

1.2. Fibre-matrix bonding

During the loading of the material, the tension at the first crack of the matrix rises to increase with the bonding and, still, with the aspect ratio and fibre concentration [9]. With the bonding increase, the elastic tensile strength also increases and sometimes the ductility reduces. As seen, the chosen tests must indicate the best option, with both high toughness and acceptable strength of composites.

1.3. Effects of ageing

Three main approaches for the improvement of vegetable fibre durability should be considered. One is based on the protection of the fibres by coating [10] or sealing the dry composite to avoid the effect of alkaline water. Another is the adoption of high casting compaction [11] and of high-pressure steam curing for providing matrix carbonation [12], if necessary adding silica fume [13]. The third approach is related to the use of low alkaline binders based on industrial and agricultural by-products [14]. For the climate conditions of São Paulo (Brazil), the suitability of coir fibre reinforced cementitious composites was attested to through the use of outdoor panels, with a cost reduction as high as 15% [15].

2. Experimental study

2.1. Materials

Ordinary Portland cement without any addition of carbonates was used, in order to avoid interference on the EDS results.

The fibres used were malva (*Urena lobata* Linn.), sisal (*Agave sisalana* Perrine), coir (*Cocos nucifera* Linn.), chrysotile asbestos and polypropylene. None of the fibres received any chemical treatment.

The asbestos fibres were of the 4Z type (Quebec screen test classification), commercially used in Brazil by the asbestos-cement industry.

Vegetable and polypropylene fibres were used in lengths that varied from 15 to 30 mm, for random distribution in the matrix. The variability of length of the vegetable fibres was very large due to the crude cutting process.

Table 1 provides data of the water absorption by vegetable fibres during the initial 24 h of immersion.

Table 1

Water absorption by vegetable fibres at room temperature. ASTM C127/88

Water absorption (% wt)							
Fibre/time	5 min	15 min	30 min	1 h	4 h	8 h	24 h
Malva	136.6	160.3	162.4	186.4	142.8	156.6	156.4
Sisal	89.3	88.4	94.7	95.4	97.0	96.8	92.2
Coir	43.2	52.9	53.0	58.3	67.9	72.2	80.4

The first 15 min is responsible for, at least, 53% of the total absorption; after 8 h of immersion, a process of stabilization is evident. This characteristic affects the effective water–cement ratio in the matrix, because part of the water is absorbed by the fibres.

The vegetable fibres were oven dried at 60°C before use. Savastano [16] did not recommend wetting fibres before use, due to the fact that the saturated dry surface condition cannot be accurately measured and consequent significant alteration of the mechanical performance of the composite may occur.

2.2. Vegetable fibres characterization

The malva fibres are removed from the bark of the stalks [17]. At present, the annual Brazilian production is about 7000 t and the main industrial use is for production of sacks. The average wholesale price of the fibre is US\$ 0.35/kg, in the field.

Sisal fibres are obtained from the leaves of the plant and the commercial fibres correspond to no more than 4% of the total leaf mass. Brazil is the largest producer of sisal in the world: 196 000 t in 1996 [18]. The price for export is US\$ 0.53/kg-FOB.

The coir fibres, which are extracted from the husk, basically from the mesocarp of the fruit, are a by-product of the coconut processing industry. As reported by Savastano et al. [19], the Brazilian production of short residual fibres (1–3 cm) is about 3000 t/yr at a price of US\$ 0.27/kg.

The main properties of the fibres are presented in Table 2. The values, compiled by Savastano et al. [20], are the average of a large number of samples with high coefficients of variation (sometimes as high as 100%).

2.3. Composite production

The matrix consisted only of Portland cement paste so as to have no interference of aggregates upon the transition zone between the fibres and the matrix. Water–cement ratios of 0.30, 0.38 and 0.46 at ages of 7, 28, 90 and 180 days were used.

Volume fraction for each fibre was determined to be a reasonable maximum without causing problems in

Table 2
Main characteristics of the fibres

Property	Coir	Sisal	Malva	Asbestos	Polypropylene
Density (kg/m ³)	1177	1370	1409	2400	913
Cellulose amount (% mass)	53.0	78.6	76.0	—	—
Lignin amount (% mass)	40.8	9.9	10.0	—	—
Elongation at break (%)	37.7	5.2	5.2	2	24.2
Tensile strength (MPa)	107	363	160	655	250
Young's modulus (GPa)	2.8	15.2	17.4	164	2.0

mixing due to balling of the fibres. The fibre volumes used were 4% for the vegetable fibres and 1% for the polypropylene and asbestos fibres.

The composite was mixed in an ordinary mortar pan mixer, casted on a vibrating table without pressure and cured in a wet chamber until the date of the test.

2.4. Experimental methods for the microanalysis

The microscopical analysis in this study was based on scanning electron microscopy (SEM), with backscattered electron image and energy dispersive spectroscopy (EDS).

Backscattered electron imaging is appropriate for sectioned specimens with a smooth, polished surface. The image is suitable for quantitative measurements of different regions by way of atomic number contrast [21].

The technique for preparing the specimens for backscattered electron image analysis and EDS was based on the Kjellsen et al.'s [22] recommendations.

The specimens were impregnated with an epoxy resin diluted in ethanol and submitted to 85 kPa vacuum for 2 min. Then the specimens were kept in an oven for 15 h to accelerate resin polymerization and later cut into standardized dimensions. The specimens were ground and polished using a series of grit sizes (85, 36, 15, 4–8, 2–4, <1 μm). After the final polishing stage the specimens were cleaned ultrasonically in acetone. The samples were carbon-coated before examination in the SEM.

3. Results of the microanalysis

The main results of this study are micrographs of fibre–cement composites (Figs 1–10) and EDS spot analysis (Table 3).

3.1. Malva–cement paste composites

In Fig. 1, the composite water–cement ratio is 0.38 and the age is 180 days. Debonding of the matrix–fibre

interface occurs due to fibre shrinkage upon drying. This kind of debonding is common in composites with vegetable fibres, and harms the adherence between the phases. The transition zone thickness is approximately

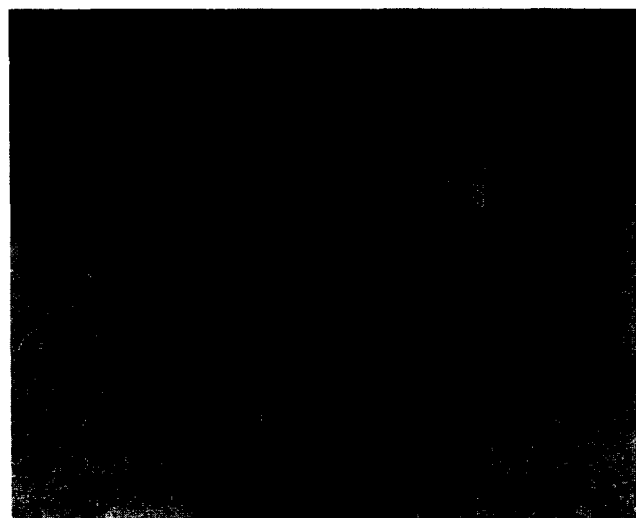


Fig. 1. BSEI. Malva fibre–cement composite, w/c = 0.38, 180 days. Arrow: portlandite macrocrystals.

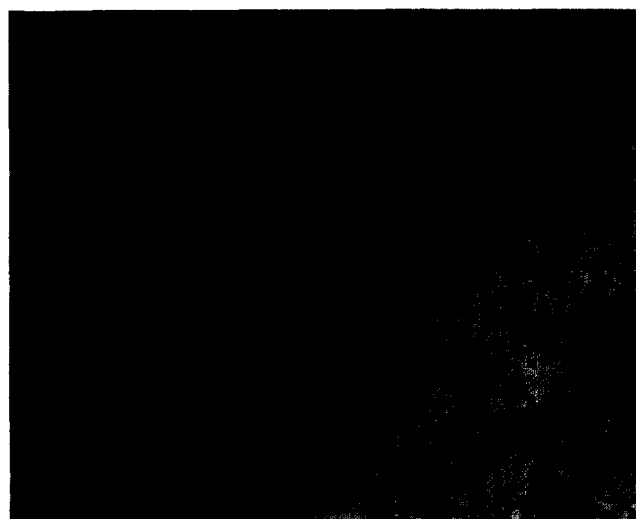


Fig. 2. BSEI. Sisal fibre–cement composite, w/c = 0.38, 7 days. Arrow: hydration products at the fibre surface.

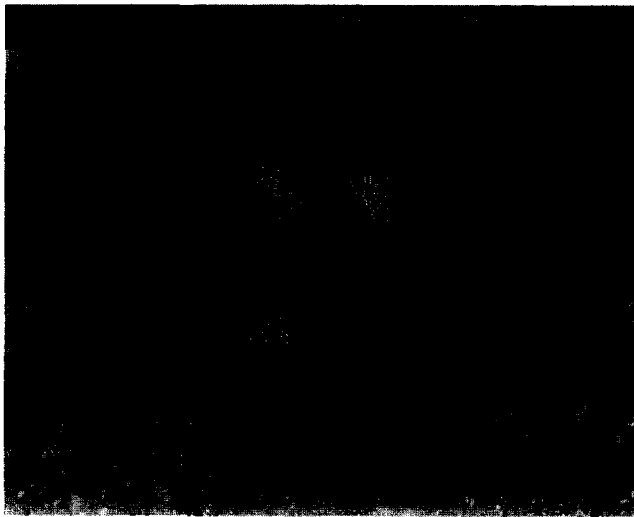


Fig. 3. BSEI. Sisal fibre–cement composite, $w/c = 0.38$, 180 days. Arrow 1: portlandite crystals; arrows 2 and 3: regions of the transition zone rich in calcium hydroxide.

50 μm , with portlandite crystals piled up (arrow); the bulk cement paste is very compact.

3.2. Sisal–cement paste composites

The composite with a water–cement ratio of 0.38 and 7 days old is presented in Fig. 2. The fibre is placed longitudinally, detached from the matrix, and the arrow indicates the place of an EDS analysis (Table 3). Hydration products are detected on the fibre surface, with low evidence of calcium hydroxide ($\text{Ca}/\text{Si} = 2.89$). The Al, Fe and Mg percentages indicate the possibility of hydrogarnet with brucite precipitation (magnesium hydroxide).



Fig. 4. BSEI. Coir fibre–cement composite, $w/c = 0.38$, 7 days. Arrow 1: debonding caused by the volume diminishing of the fibre; arrow 2: fissure deviated by the fibre, crossing the transition zone.

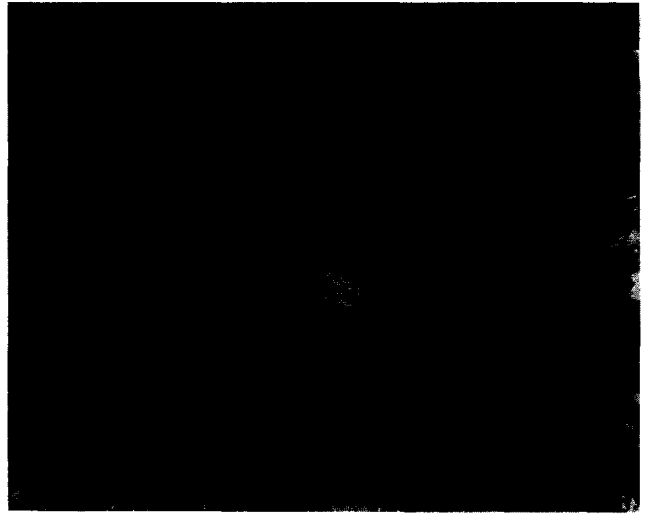


Fig. 5. BSEI. Coir fibre–cement composite, $w/c = 0.38$, 28 days. Arrow: portlandite accumulation with thickness of up to 20 μm .

Figure 3 shows the same composite 180 days old. The transition zone thickness is about 200 μm , porous and rich in calcium. Two EDS analyses indicate Ca/Si ratios of 6.31 and 4.39, respectively, as can be seen in Table 3, and there is a portlandite crystal region, in platelike layers and with a dimension greater than 70 μm (arrow 1).

For the vegetable fibres, the high porosity induces the formation of large crystals of portlandite, that do not form on the fibre surface, but in the transition zone interior.

3.3. Coir–cement paste composites

In Fig. 4, there is a backscattered electron image of the composite with a water–cement ratio of 0.38 at

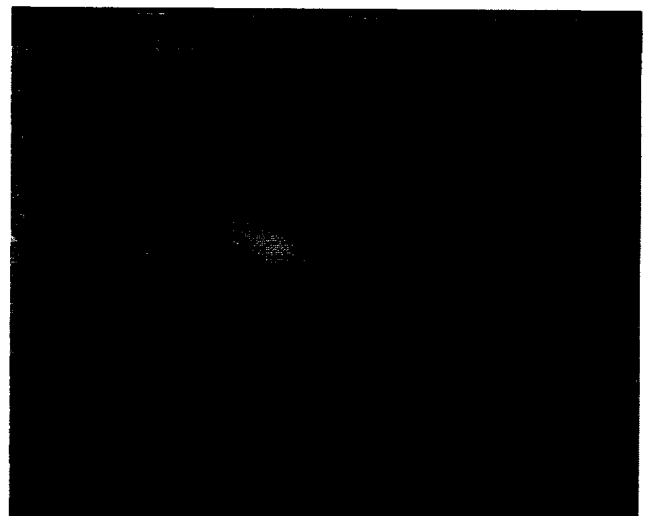


Fig. 6. BSEI. Coir fibre–cement composite, $w/c = 0.46$, 28 days. Arrow: large portlandite crystals, with thickness of up to 40 μm .



Fig. 7. BSEI. Asbestos fibre–cement composite, $w/c = 0.38$, 28 days. Arrow: 'T' shaped fissure deviated by the fibre.



Fig. 9. BSEI. Polypropylene fibre–cement composite, $w/c = 0.30$, 28 days. Arrow: film of hydrated products.

7 days of age. The bulk cement paste shows a very loosely compacted hydrated structure (dark points) and high proportions of unhydrated grains (light grey regions), with a dimension about $35\text{ }\mu\text{m}$, due to the low hydration age. Debonded fibres can also be seen (arrow 1) and the crack evolution through the transition zone (arrow 2) indicates low strength.

With reference to Fig. 5 (water–cement ratio of 0.38 and 28 days old), the EDS analysis (Table 3) indicates the heterogeneous distribution of portlandite crystals in the transition zone: the regions marked by the arrow show a very high Ca/Si ratio (7.52) and in another dark point, at left, the ratio is lower (3.25).

The composite with water–cement ratio of 0.46 at 28 days shows a great accumulation of portlandite close

to the fibres. Figure 6 shows microcracks that follow the outlines of the calcium hydroxide crystals.

3.4. Asbestos–cement paste composites

Figure 7 shows the backscattered electron image in a water–cement matrix of 0.38 at 28 days of age. The crack, in the shape of a 'T', suffers a bifurcation as it crosses the fibre, which represents the principal factor of the increase of fracture energy by the composite, compared with the matrix without fibres. Agglomerations of fibres form dark regions in the micrographs, due to the increased porosity. Asbestos fibres, basically constituted of silicon and magnesium, can be hard to see in the micrographs due to lack of contrast.



Fig. 8. BSEI. Asbestos fibre–cement composite, $w/c = 0.46$, 28 days. Arrows 1 and 2: fissure crossing the fibre agglomeration; arrow 3: portlandite crystals.



Fig. 10. Polypropylene fibre–cement composite, $w/c = 0.38$, 180 days. Porous transition zone and fissure dislocated by the fibre.

Table 3
Spot analysis by energy dispersive spectroscopy (EDS)

Composite			Fig. of reference (no.)	Atomic %								(Ca/Si) ratio	Observations about analysed region
Fibre	w/c ratio	Age (days)		Ca	Si	Mg	Al	S	Fe	K	P		
Sisal	0.38	7	[2]	59.392	20.576	5.622	7.942	0.232	4.638	1.598	0.000	2.89	Arrow. Hydration products at the fibre surface. High porosity.
Sisal	0.38	180	[3]	69.539	11.026	5.220	6.448	3.242	3.862	0.663	0.000	6.31	Arrow 2. Transition zone rich in portlandite.
Sisal	0.38	180	[3]	51.963	11.840	17.232	10.095	4.984	2.882	1.004	0.000	4.39	Arrow 3. Transition zone rich in portlandite, with high porosity.
Coir	0.38	28	[5]	83.308	11.079	2.586	1.740	0.000	1.081	0.206	0.000	7.52	Arrow. Transition zone rich in portlandite
Coir	0.38	28	[5]	64.822	19.921	7.081	3.491	0.000	3.146	1.539	0.000	3.25	Porous transition zone, without concentration of portlandite crystals.
Asbestos	0.46	28	[8]	98.774	0.701	0.081	0.081	0.002	0.190	0.000	0.171	140.90	Arrow 3. Macrocrystals of portlandite.

In Fig. 8, the composite has a water–cement ratio of 0.46 and 28 days of age. The transition zone is porous, rich in calcium hydroxide and microcracked. Near the fibres, due to the availability of space and water, there are large portlandite nuclei, formed by a through-solution hydration process. Arrow 3 shows the EDS analysis position and the result shown in Table 3 reveals the almost exclusive occurrence of calcium hydroxide.

3.5. Polypropylene–cement paste composites

Figure 9 presents the backscattered electron image of a composite 28 days old and water–cement ratio of 0.30. Debonded zones are almost non-existent, because the fibres do not suffer shrinkage, and that ensures adherence and energy absorption during the composite cracking. The fibre is seen on the top, surrounded by a film of hydration products, with a width of approximately 1 μm . At the time of the present study the film formation was only observed in polypropylene–cement composites.

Figure 10 illustrates a composite with a water–cement ratio of 0.38 at 180 days. Another typical situation of the reinforcement of polypropylene fibres is seen: the fibre deviates the crack and this interferes to a great extent in the process of energy dissipation and helps to increase the composite ductility.

4. Main results of mechanical tests

As initially presented elsewhere [23,24], the four point bending test was adopted, following a RILEM

recommendation [25] for testing cement composites. The specimens were small beams, 300 mm long, with a cross-section of 150 \times 15 mm tested over a span of 270 mm. Figure 11 presents the specific energy as a function of age. Specific energy is defined as the total energy absorbed by the fractured surface. As expected, the short asbestos fibres induced a small increase in energy absorption. The best results were obtained with the polypropylene fibres. The vegetable fibre composites performed satisfactorily in comparison with asbestos and non-reinforced matrices.

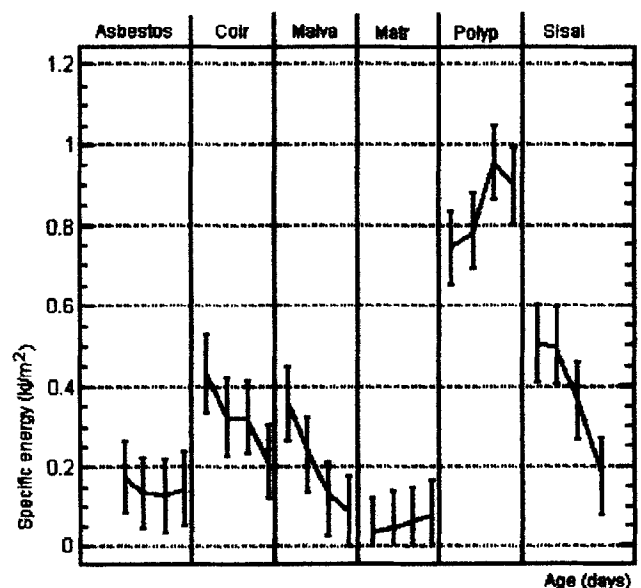


Fig. 11. Bending test: effect of the age on specific energy with water–cement ratio of 0.38; for each fibre, the age sequence is 7, 28, 90 and 180 days.

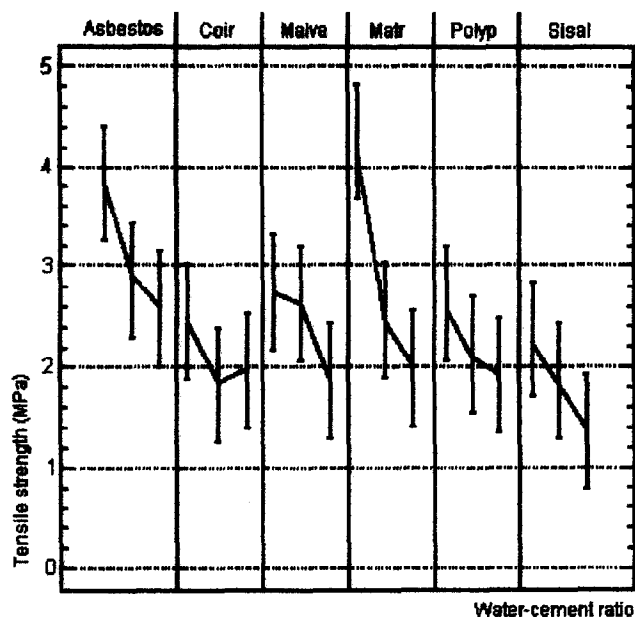


Fig. 12. Direct tensile test: effect of water–cement ratio on the strength at the age of 28 days; for each fibre, the w/c sequence is 0.30, 0.38 and 0.46.

The effect of ageing has been observed in composites with vegetable fibres, which present a reduction of ductility with an increase in age because of deterioration of the fibres in an alkaline medium.

The ASTM C 190 test method for mortars was also applied for the composites. In Fig. 12, as expected, tensile strength is reduced with an increase of the water–cement ratio. The best results are achieved with asbestos fibres, probably due to the dense transition zone (Fig. 7).

5. Discussion

Scanning electron microscopy (SEM) with backscattered electron imaging, as has been observed by Scrivener [26], permits a better transition zone characterization, when compared with secondary electron imaging.

5.1. Comparison of vegetable fibres with asbestos

For composites with impermeable asbestos fibres, a wall effect occurs, wetting the fibres surface with a water film. This factor is principally responsible for the formation of a transition zone as can be observed in Fig. 8. Akers and Garrett [27], in a study of asbestos fibre reinforced cement, used the technique of pressurization during the moulding that, added to the large specific area of asbestos fibres, avoids their complete wetting. This technique, despite difficult in execution, diminishes the porosity and does not induce the forma-

tion of portlandite macrocrystals at the asbestos fibre surroundings.

The vegetable fibres present a water absorption rate greater than 80%, which inhibits the wall effect and produces a strong flow of water in the direction of the fibre. This fact induces a local increase of the water–cement ratio, and causes high porosity in the transition zone, whose thickness varies between 50 and 100 μm . This should be the opposite of the expectation if compared with porous aggregate [3,28] but one must have in mind that fibres are discrete and widespread in the matrix and with a large capacity of water attraction: the high porosity in the transition zone seems to be greater with malva and sisal fibres (Figs 1 and 3), which present at least 95% of water absorption at the first 30 min.

EDS analysis confirms the presence of portlandite macrocrystals, whose growth is due to the greater mobility of calcium ions in a water environment. Coutts and Ni [29] and Zhu et al. [30] also proposed the process of pressure moulding for composites with vegetable fibres, which reduces the water–cement ratio but increases the cost of component production. In this way, when the pressure is removed, the saturated fibre releases the absorbed water back to the matrix. Coutts [31] also proposed that it was possible to get a dense transition zone and of little thickness, contrary to the observations in this study. The increase of costs during production determined by the adoption of pressure, dewatering and autoclave processes seems to be justified by the better performance of composites.

Another observation made from Figs 1–8, is that the fibrillated aspect of the malva and asbestos fibres induces agglomerations in the interior of the matrix, a fact that contributes to the increase of entrapped air voids and to a consequent reduction in the fibres' adherence.

5.2. Comparison of vegetable fibres with polypropylene

The impermeable fibres of polypropylene present the wall effect and, as the filaments have a smooth surface, it is possible in some cases to visualize a discontinuous film of hydrated products on the fibre surface, with a thickness of approximately 1 μm (Fig. 9). The transition zone is nearly as dense as the matrix, with a thickness of no more than 20 μm and small occurrence of portlandite. These results are similar to those presented by Bentur et al. [32], for polypropylene fibres reinforced concrete, which gives additional support for the experimental procedures adopted by the present research.

The dimensional variation of vegetable fibres, which is due to the elevated water absorption, mainly for malva and sisal fibres (see Table 1), produces insufficient bonding and therefore their performance is not as

good as with polypropylene fibres, as can be seen in Fig. 10.

6. Conclusions

The transition zone presents a different aspect from the rest of the matrix, related to the following main points:

- Thickness of up to 100 μm , that may be identified by matrix cracking and by the localized increase of porosity and portlandite concentration, principally when vegetable fibres are used without special casting procedures.
- Influence of the water–cement ratio; higher values induce an increase in the thickness of the transition zone and/or the higher accumulation of portlandite crystals without any defined arrangement.
- Higher porosity of the matrix near the interface at the initial ages of hydration.

Based on these aspects, a correlation between the interfacial characteristics and the bulk properties is proposed:

- Excessive porosity of the vegetable fibres, which contributes to the inferior macrostructural performance of the composites. During the mixing of the composite, the porous vegetable fibres attract a great quantity of water, making the transition zone more pronounced than when asbestos or polypropylene fibres are used.
- The fibre debonding from the matrix must be the result of its great shrinkage. The main effect of this phenomenon is the low energy absorption during mechanical test and so a factor to the reduction of the ductility of the composite.
- The fibre decay is more evident with the increase of the age. Therefore the fibre itself becomes probably the weakest part of the composite and another reason to the reduction of the ductility of the composite.

The transition zone characteristics constitute important elements to make practical the application of fibre reinforced materials, especially for hydraulic cements reinforced with vegetable fibres, and the present major task is to improve this zone without significantly increasing the cost of building component production.

Acknowledgements

The authors are especially grateful to the Instituto de Pesquisas Tecnológicas do Estado de São Paulo, where the specimens were prepared for the experiments, and to Professor Paulo Sergio C. Pereira da

Silva, who co-ordinated the operation of the scanning electron microscope at the Department of Metallurgy and Materials Engineering of the Escola Politécnica of the University of São Paulo. They are also indebted to Dr Maria A. Cincotto, Dr David Lange, Mr Pedro C. Bilesky and Ms Denise S. Ablas for their help with this research.

References

- [1] Mindess S, Odler I, Skalny J. Significance to concrete performance of interfaces and bond: challenges of the future. In: *Proceedings of the 8th International Congress on the Chemistry of Cement*, Abla, Rio de Janeiro, 1986;1:151–7.
- [2] Wei S., Mandel J.A., Said S. Study of the interface strength in steel fiber-reinforced cement-based composites. *ACI Journal* 1986;83(4):597–605.
- [3] Zhang M.-H., Gjorv O.E. Microstructure of the interfacial zone between lightweight aggregate and cement paste. *Cement and Concrete Research* 1990;20(4):610–618.
- [4] Savastano Jr H, Agopyan V. Transition zone of hardened cement paste and vegetable fibres. In: Swamy RN, editor. *Proceedings of the 4th International Symposium of Fibre Reinforced Cement and Concrete*. London: E and FN Spon, 1992:1110–9. (RILEM Proc., 17)
- [5] Monteiro PJM. Microstructure of concrete and its influence on the mechanical properties. PhD thesis, University of California, Berkeley, 1985.
- [6] Majumdar A.J., Ryder J.F. Reinforcement of cements and gypsum plasters by glass fibres. *Science of Ceramics* 1970;5:539–564.
- [7] Bentur A., Diamond S., Mindess S. Cracking process in steel fiber reinforced cement paste. *Cement and Concrete Research* 1985;15(2):331–342.
- [8] Bentur A., Akers S.A.S. The microstructure and ageing of cellulose fibre reinforced cement composites cured in a normal environment. *The International Journal of Cement Composites and Lightweight Concrete* 1989;11(2):99–109.
- [9] Gray R.J. Analysis of the effect of embedded fibre length on fibre debonding and pull-out from an elastic matrix — part 2: application to a steel fibre–cementitious matrix composite system. *Journal of Materials Science* 1984;19(5):1680–1691.
- [10] Guimaraes SS. Vegetable fiber–cement composites. In: Sobral HS, editor. *Proceedings of the 2nd International Symposium on Vegetable Plants and their Fibres as Building Materials*. London: Chapman and Hall, 1990:98–107. (RILEM Proc., 7).
- [11] Aggarwal L.K. Bagasse-reinforced cement composites. *Cement and Concrete Composites* 1995;17:107–112.
- [12] Soroushian P., Shah Z., Won J.-P. Aging effects on the structure and properties of recycled wastepaper fiber cement composites. *Materials and Structures/Materiaux et Constructions* 1996;29:312–317.
- [13] Gram HE. Durability of natural fibres in concrete. In: Swamy RN, editor. *Natural fibre reinforced cement and concrete*. Glasgow: Blackie, 1988:143–72. (Concrete and Technology Design, 5).
- [14] John VM, Agopyan V, Derolle A. Durability of blast furnace-slag-based cement mortar reinforced with coir fibres. In: Sobral HS, editor. *Proceedings of the 2nd International Symposium on Vegetable Plants and their Fibres as Building Materials*. London: Chapman and Hall, 1990:87–97. (RILEM Proc., 7).
- [15] Agopyan V., John V.M. Durability evaluation for vegetable fibre reinforced materials. *Building Research and Information* 1992;20(4):233–235.

- [16] Savastano Jr H. The use of coir fibres as reinforcement to Portland cement mortars. In: Sobral HS, editor. *Proceedings of the 2nd International Symposium on Vegetable Plants and their Fibres as Building Materials*. London:Chapman and Hall, 1990:150–7. (RILEM Proc., 7).
- [17] Agopyan V. Vegetable fibre reinforced building materials — developments in Brazil and other Latin American countries. In: Swamy N, editor. *Natural fibre reinforced cement and concrete*. Glasgow:Blackie, 1988:208–42.
- [18] Food and Agriculture Organization of the United Nations (FAO) — Committee on commodity problems — Intergovernmental group on hard fibres. *Sisal and henequen:summary note on developments in 1995 and 1996*. Manila:FAO, 1996 (CCP:HF 96/2).
- [19] Savastano Jr H, Nolasco AM, Oliveira L. Disponibilidade de residuos de alguns tipos de fibra vegetal, no Brasil, para uso em componentes de construcao. In: *Memorias del Seminario Iberoamericano de Materiales Fibrorreforzados*, Cytel PIP VIII.5, Cali: Universidad del Valle/Cytel, 1997:128–132. (Articulo 16).
- [20] Savastano Jr H, Dantas FAS, Agopyan V. Materiais reforçados com fibras:correlacao entre a zona de transicao fibra-matriz e as propriedades mecanicas. Sao Paulo:IPT/Pini, 1994. (Publicacao IPT 2158 — Boletim 67).
- [21] Goodhew PJ, Humphreys FJ. *Electron microscopy and analysis*, 2nd ed. London:Taylor and Francis, 1988.
- [22] Kjellsen K.O., Detwiler R.J., Gjorv O.E. Backscattered electron image analysis of cement paste specimens:specimen preparation and analytical methods. *Cement and Concrete Research* 1991;21(2/3):388–390.
- [23] Agopyan V, Savastano Jr H. Fibre–cement paste transition zone. In: Diamond S, et al., editors. *Proceedings of Materials Research Society Symposium on Microstructure of Cement-based Systems/Bonding and Interfaces in Cementitious Materials*, Boston, 1994:479–86 (MRS Symp Proc. Vol. 370).
- [24] Savastano Jr H, Agopyan V, Dantas FAS. Fibre–cement paste transition zone:characterisation and effect on the mechanical properties. In: *Proceedings of the RILEM International Conference on Interfaces in Cementitious Composites*, Toulouse, 1992. London:E and FN Spon, 1993:23–32.
- [25] Reunion Internationale des Laboratoires D'Essais et des Recherches sur les Materiaux et les Constructions (RILEM), *Testing methods for fibre reinforced cement-based composites. Materiaux et Constructions* 1984;17(102):441–56. (RILEM Draft Recommendations, Technical Committee 49 TFR).
- [26] Scrivener KL. The microstructure of concrete. In: Skalny JP, editor. *Materials science of concrete I*. Westerville:American Ceramic Society, 1989:127–61.
- [27] Akers S.A.S., Garrett G.G. Fibre-matrix interface effects in asbestos–cement composites. *Journal of Materials Science* 1983;18(7):2200–2208.
- [28] Zhang M.-H., Gjorv O.E. Penetration of cement paste into lightweight aggregate. *Cement and Concrete Research* 1992;22(1):47–55.
- [29] Coutts R.S.P., Ni Y. Autoclaved bamboo pulp fibre reinforced cement. *Cement and Concrete Composites* 1995;17:99–106.
- [30] Zhu W.H. et al. Air-cured banana-fibre-reinforced cement composites. *Cement and Concrete Composites* 1994;16:3–8.
- [31] Coutts R.S.P. Fibre-matrix interface in air-cured wood-pulp fibre–cement composites. *Journal of Materials Science Letters* 1987;6(2):140–142.
- [32] Bentur A, Mindess S, Skalny J. Reinforcement of normal and high strength concretes with fibrillated polypropylene fibres. In: Swamy RN, Barr B, editors. *Proceedings of the International Conference on Recent Developments in Fibre Reinforced Cements and Concretes*. Barking:Elsevier, 1989:229–39.